Polyaniline/Pillared Montmorillonite Clay Composite Nanofibers

N. Narayanan Binitha, Sankaran Sugunan

Department of Applied Chemistry, Cochin University of Science and Technology, Kochi-682 022, India

ABSTRACT: *In situ* polymerization of aniline is done inside the pillared clay matrix. The nonswellable pillared clay confined matrix allows efficient polymerization that leads to nanofibrous morphology. As a result high polymer order and crystallinity is attained and is evident from XRD patterns. The strong interaction between the clay layers and polyaniline (PANI) is understood from FTIR and DRS spectra. Additionally these analytical results suggest that the prepared PANI is in the doped state. The PANI/pillared clay nanocomposite formation gives additional thermal stability to the polymer backbone and is clear from the DTG curves. © 2007 Wiley Periodicals, Inc. J Appl Polym Sci 107: 3367–3372, 2008

Key words: pillared montmorillonite; polyaniline; composites; nano fibers; thermogravimetric analysis

INTRODUCTION

Polyaniline (PANI) – nanocomposites are industrially important due to the additional thermal and mechanical strength as well as the processability offered to PANI in the conducting form. Among the conducting polymers, PANI is popular due to its environmental stability, easiness and low cost of preparation, unique redox properties[1] and high conductivity.[2] A wide range of potential applications are explored for PANI. PANI composite systems can provide new synergistic properties that cannot be attained from individual materials.[3,4] Among the inorganic materials for hybrid composite formation, the small particle size and ease of intercalation gives attention to montmorillonite clays.[5] One-dimensional PANI nano structures have received great attention because of their unique properties and applications in electrical nano devices.[6]

Many articles are there on PANI – montmorillonite composites,[7–13] to the best of our knowledge no paper dealing with PANI – montmorillonite composite nanofibers have been published yet. This may be due to a low amount of exfoliation occurring to silicate layers. Eventhough there is intercalation, the Van der Waals forces binding the clay layers are weak and in aqueous solution, the layers swells and some silicate layers may become exfoliated. Commonly used method to prepare the nanocomposite is intercalation of aniline into the gallery of clay layers followed by *in situ* polymerization.[14,15]

We have successfully synthesized PANI composite nanofibres through *in situ* polymerization of aniline inside the matrix of pillared montmorillonite. Jagtap N and Ramaswamy V had reported oxidation of aniline over titania pillared montmorillonite clays.[16] Here the oxidant selected is H_2O_2 that resulted in the selective formation of azoxybenzene at room temperature, whereas in the present work $(NH_4)_2S_2O_8$ as the initiator oxidant provided oxidative polymerization of aniline in acidic medium at a low temperature. Pillaring of montmorillonite results in enhanced interlamellar distance and the force acting between the clay layers become covalent upon pillaring.[17] This may result in increased intercalation of aniline into the matrix and polymerization occurs in the confined environment to give nanofibers. Pillared interlayered clays (PILC) are two-dimensional zeolites like materials prepared by exchanging the charge compensating cations between the smectite clay layers by partially hydrated polymeric or oligomeric cation complexes in the interlamellar region of the clay, drying and calcining transforms the metal polyoxocations into metal oxide pillars which results in high porosity, surface area, and acidity.[18] Present study uses pillaring with polyoxocations of chromium to get chromia pillared montmorillonite for PANI–PILC nanocomposites preparation.

EXPERIMENTAL

Materials

The materials used, montmorillonite, KSF (Aldrich), chromium nitrate (CDH), sodium nitrate (Merck), so-

dium carbonate (Sd Fine Chemicals), aniline (Merck), hydrochloric acid (Qualigens), ammonium peroxodisulfate (Qualigens), methanol (Sd Fine Chemicals), and acetone (Sd Fine Chemicals) are of high purity and used as it received.

Pillared montmorillonite preparation

Chromia pillaring is done on Na^+ exchanged montmorillonite clay using the procedure reported by T.J. Pinnavaia[19] with slight modifications. We have selected the pillaring solution to clay ratio as 10 mmol metal/g clay. Na^+ exchange is done by treatment of KSF with $0.5M$ sodium nitrate solution for 24 h at 70°C then filtered, made nitrate free by washing, and is dried at 110°C. This is then used in pillaring following the reported procedure.[19]

About $0.2M$ solution of chromium nitrate was partially hydrolyzed by drop wise addition of $0.3M$ sodium carbonate (Sd Fine Chemicals) solution with a base to metal ratio of 2 under vigorous stirring for 2 h at 95°C and is again stirred at the same temperature for 6 h. This pillaring solution is then added to the previously swelled sodium exchanged montmorillonite clay. The solution is stirred at 70°C for 24 h, kept overnight, filtered, washed free of nitrate ions, dried at 110°C, and calcined at 500°C for 5 h to get chromia pillared montmorillonite. The pillared clay is designated as PILC.

Preparation of PANI–PILC nanocomposites

The nanocomposites are prepared by *in situ* intercalative polymerization of aniline. The PILC is added to $1M$ HCl aqueous solution and is stirred for 1 h. Aniline monomer is then added to this colloidal suspension of clay in a ratio of 50 mmol aniline/g clay (4.65 g aniline/g clay), stirred for the intercalation of aniline into the silicate layers, and is kept at 0°C. Ammonium persulfate, $(NH_4)_2S_2O_8$, dissolved in $1M$ HCl is added slowly to solution containing aniline and PILC at an aniline/oxidant molar ratio of 1 : 1.25, then stirred for 8 h and is kept overnight. The nanocomposites is separated by filtration and washing with acetone, methanol, and distilled water. This is done to remove oligomers, excess oxidant and residual aniline monomer. The composite is dried at 50°C. The prepared nanocomposites are designated as PANI – PILC.

Characterization

The surface morphologies of PANI/clay nanocomposites are taken in a JSM – 840 A, Scanning electron microscope, JEOL – Japan. The basal spacing of the nanocomposites is measured using an X-ray diffrac-

tometer using a Rigaku D MAX III VC Ni-filtered Cu Kα radiation ($\lambda = 1.5404$ Å at a scan rate of 4°/min). FTIR spectra are obtained by the KBr pellet method on ABB BOMEM (MB Series) spectrometer in the range 400–2800 cm^{-1}. UV–vis spectra of PANI/PILC nanocomposites were taken in the range 200–800 nm on an Ocean Optics. SD 2000, Fiber Optic Spectrometer equipped with a diffuse reflectance attachment, with a charged coupled device detector at room temperature using MgO as the reference; the samples are flushed with an inert atmosphere. The electrical conductivity of PANI/PILC nanocomposites was measured in a compressed pellet (1.5 cm diameter – 0.05 cm thick) at room temperature by the four-probe technique using an electrometer. Thermogravimetric analysis (TGA/DTG) was carried out in a Perkin Elmer Pyris Diamond thermogravimetric/differential thermal analyzer by heating the sample at a rate of 20°C min^{-1} from room temperature to 800°C in air.

RESULTS AND DISCUSSION

Morphology

SEM photographs in Figure 1 shows the nanofibrous morphology of PANI in the clay matrix. The layered structure of the clay is evident from the picture. Figure 1(a,c) represents the fibrous PANI composites and Figure (b) shows the PILC. The enhanced layer distance in PILC allows the intercalation of more monomers and efficient polymerization occurs within the layers. Since in PILCs the further layer expansion in polar medium is absent (swelling properties are lost[20]), which is found in montmorillonite, there is no chance of exfoliation. In PILCs, the bonding between the layers is covalent and the polymerization occurs within the confined media and as a result, polymer with high crystallinity and polymer order are expected. This explains the nanofiber formation. Note that traditional chemical polymerization using common mineral acids yields granular PANI.[21,22] Thus the morphology of the composite seen from SEM photographs suggests polymer intercalation. The nanofiber formed within the clay layers may be molecule fiber of doped PANI. Molecular models and crystal structure studies of emeraldine. HCSA (PANI doped with D,L-camphorsulfonic acid)[23] synthesized by surfactant-assisted chemical oxidative polymerization of aniline in dilute aqueous organic acids shows that the ''diameter'' of a single chain (molecule fiber of doped PANI) is in the range 1.0–1.8 nm. PANI nanofibers obtained in that study are chemically robust nanofibers having average fiber diameter in the range 30–50 nm and they deform readily under mechanical stress and fragment to smaller pieces (of fiber diameter 1.0–1.8 nm)
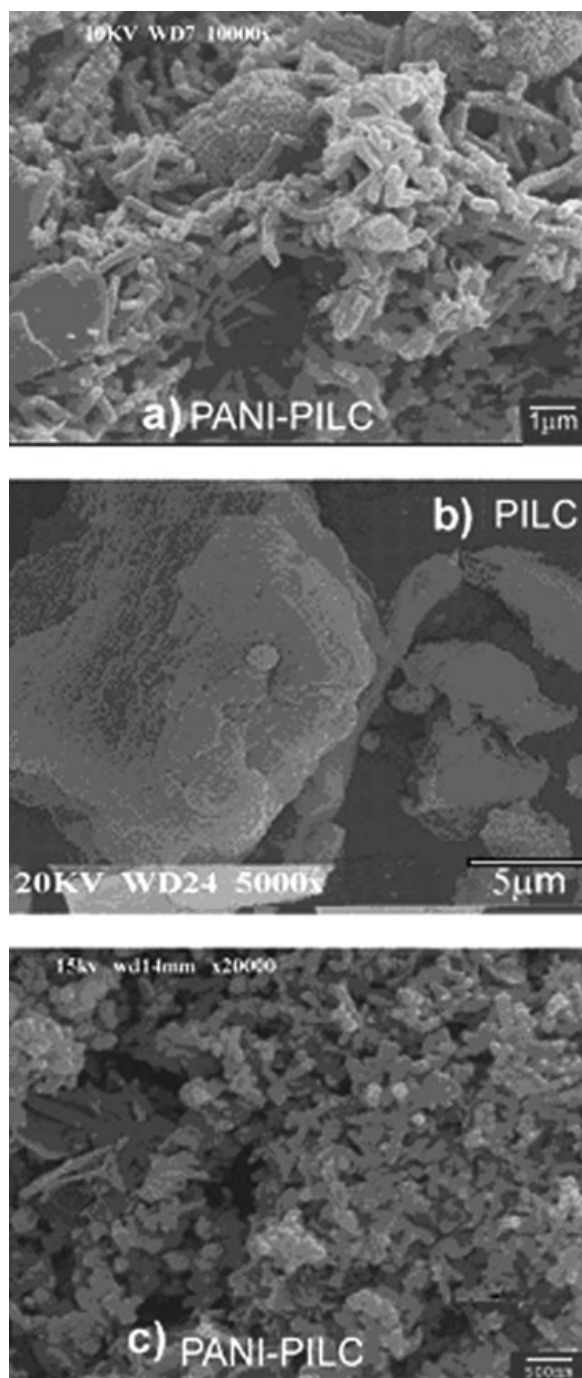
Figure 1 SEM photographs of PILC and PANI-PILC nanocomposite.

under strong probe sonication. SEM pictures in the present study show that diameter of the PANI fibers are between 100 and 300 nm. We suggest aggregation of the single PANI chains as it emerges out the clay layers. It is reported that one nanofiber contains lots of PANI chains. In HCl doped PANIs Cl^- ions have small size. Then the interchain separation may be small, resulting in an existence of strong coherence/coupling between the chains.[24,25]

XRD and FTIR analysis

From XRD patterns, the well ordered polymer within the clay matrix having high crystallinity is clearly evident. The peak centered at around $2\theta = 20°$ and $25°$ may be ascribed to the periodicity parallel and perpendicular to the polymer chain, respectively. The peak at around 2θ is $\sim 15°$, $20°$, and $25°$ are assigned to emeraldine structure.[26] The peak of 2θ is $\sim 25°$ is stronger than that of 2θ is $\sim 20°$ and is similar to the highly doped emeraldine salt.[27] The high level of crystallinity and additional peaks at 2θ values (in degrees) of 26.6, 38.0, 44.4, 47.4, and 64.9 are seen from Figure 2. These peaks are found to be absent in the PILC and thus is confirmed to be that of PANI formed. These peaks are not found over the composites prepared with unmodified montmorillonite using the same method. The XRD pattern of the composite retains all peaks present in the clay (2θ = 4.5, 18.1, 19.8, 20.7, 27.1, 28.2, 34.78, 36.58, 45.8, 50.6, 55.3, 62.0, 65.6 degrees) with decrease in intensity, showing that the basic clay layer structure is retained even after the composite formation. The position of the diffraction peak of the (100) plane defined the interlayer space in montmorillonite clays. In parent montmorillonite clay the 2θ value corresponding to the (100) plane lies at $\sim 8.9°$, with a basal spacing of 9.8 Å calculated from Bragg equation. Pillaring process results in shift of this 2θ value towards left and the increased d-spacing upon pillaring is calculated from Bragg equation.[16] The reflection corresponding to the (100) plane whose 2θ value
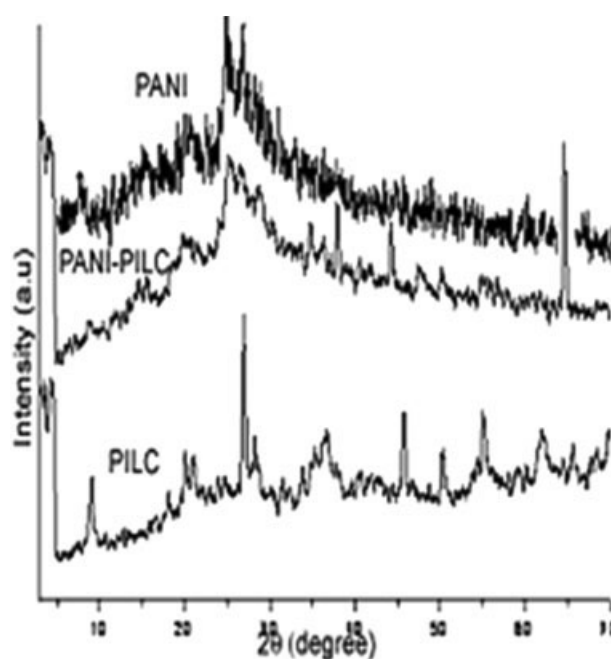

Figure 2 XRD patterns of PILC and PANI-PILC nanocomposite.
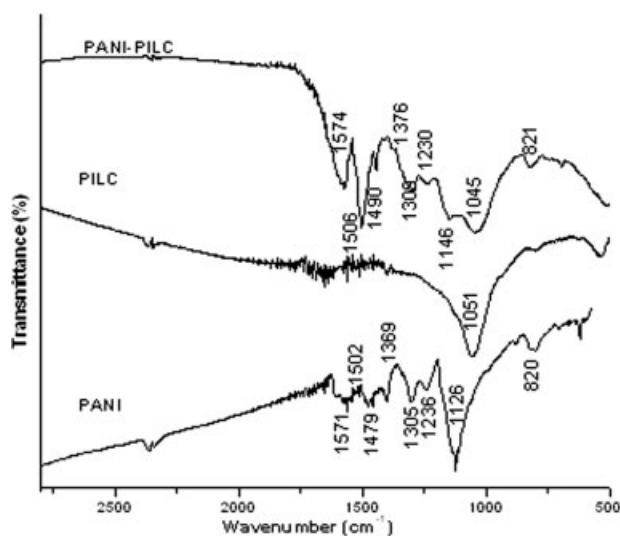
Figure 3 FTIR spectra of clay and composite.

is shifted (from 8.9° in montmorillonite towards left) after pillaring process as a result of the enhanced layer distance (d spacing = 19.6 Å) remains unaffected after composite formation. This indicates that the dimension of PANI formed inside the matrix is of nano range (<19.6 Å). The insertion of PANI is suggested from its highly crystalline nature which is not attainable without any intercalation. The absence of further enhancement in layer distance after composite formation unlike in other PANI/clay composites[7–13] may also be due to the reason that, in PILCs the bonding between layers is nearly covalent unlike in montmorillonite which is ionic or Van der Waals interaction.[16]

FTIR of PANI composite fibers exhibits absorption peaks due to the benzenoid ring of PANI at 1506, 1444, and 821 cm^{-1}. Peaks at 1574 and 1172 cm^{-1} correspond to quinoid ring[28] (Fig. 3). The Si—O—Si stretching frequency of the clay matrix (1051cm^{-1} slightly shifted to 1045 cm^{-1}) present in the composite confirms the retention of basic clay structure.[17] The peaks at 1230 and 1309 cm^{-1} originate from the aromatic amine nitrogen (C—N stretching vibrations) associated with the oxidation or protonation states in PANI.[29] In the composite there is slight shift to the frequency towards higher wave numbers and is suggested to be due to the Coulomb interaction between the positive nitrogen of the intercalated PANI and the partially negatively charged clay layers.[30]

UV–vis diffuse reflectance spectral analysis

Figure 4 shows the diffuse reflectance spectra of PANI/PILC, PANI, and PILC. PANI/PILC shows peaks due to π-π* (371 nm) and polaron-π* (458 nm).

The results suggest that the prepared PANI is in the doped state.[31,32] The incorporation of Cr^{3+} ion in the pillar position leads to characteristic absorption of light in the UV region of the DRS spectra. The Cr^{3+} ion with 3d^3 configuration is known to exhibit strong optical absorption in the UV region of the electronic spectrum. On nanocomposites formation the UV absorption around 360 nm present in PILC is strengthened, and is due to the overlap of peaks of π-π* transitions in PANI with the d–d transitions of chromium ions present in the clay. This result indicates that there is strong interaction between PANI and PILC. In bulk PANI a strong absorption peak generally appears in 780–826 nm as a result of π-polaron transitions.[27,28] But in the hybrid nanocomposites this peak is not sharp and is broadened. The broad absorption around 750 nm is a characteristic band of the polaron of PANI – emeraldine salt, formed by the head to tail coupling of the Anilinium radical.[33] The broadening may be due to the shift of peak towards near IR region[34] (free-carrier tail,[35] in the higher wavelength region). It is consistent with the delocalization of electrons in the polaron band promoted by an extended conformation of the polymer chains. Inside the clay layers, which are apart in the nanometer scale, the interaction of different polymer chains are eliminated and the chain contraction is limited. This strengthens the interaction between the polarons, and the polaron bands become more dispersed in energy. This explains the presence broad bands where polaron transitions are present.[36]

Thermal properties

Figure 5 shows the DTG curves for PANI, PILC, and the PANI-PILC composite. The composite shows a four step weight loss, as can be seen from the four
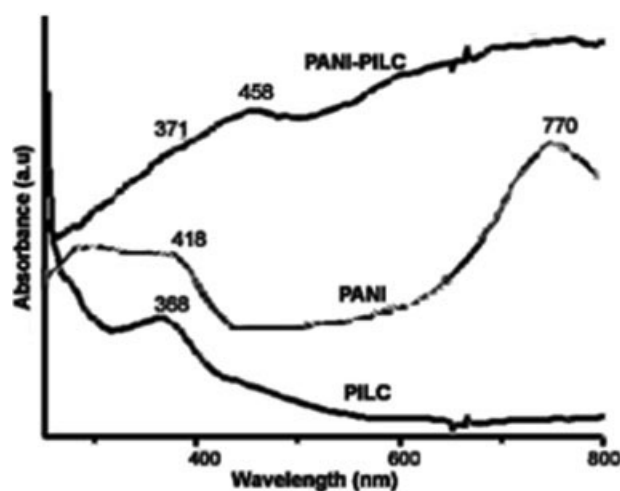

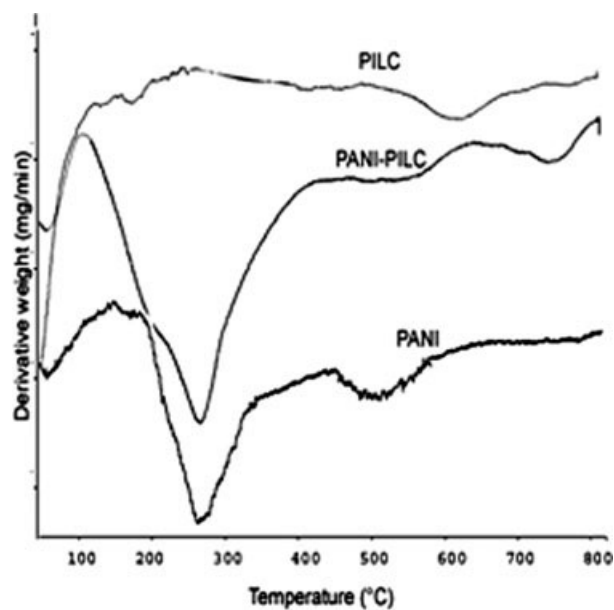**Figure 4** DRS of PILC and PANI-PILC nanocomposite.

Figure 5 DTG of clay and nanocomposite.

minima in the DTG curve indicating the majority weight loss for respective steps. The first weight loss just below 100°C is attributed to the loss of water from PANI as well as from the interlayer galleries of clay. The second weight loss ranging from 200 to 300°C, centered at 275°C is due to the elimination of dopant HCl present.[37,38] The polymer backbone breakage for pure PANI (ES) is at 523.4°C. In composite this is shifted to 579.2°C, a higher temperature by about 55.8°C, which may be due to the additional stability inside the matrix as a result of restricted motion. The weight loss around 630°C seen in the PILC DTG is attributed to the dehydroxylation of silicate structure,[39] loss of water from the interlayer galleries results in a weight loss just below 100°C. The fourth weight loss in the composite occurs at 763.3°C, which may be due to the silicate layer dehydroxylation. This result suggests that the intercalated nanocomposites system is more thermally stable, i.e., upon nanohybrid formation the stability of organic as well as inorganic material is enhanced.

The conductivity of PANI–PILC composite measured through four-probe method show a high conductivity of 3.7×10^{-2} Scm^{-1}, and is found to be comparable with the PSSA-g-PANI/montmorillonite composite that contains 13% clay.[40] Present study has 19% clay in the composite.

CONCLUSIONS

A simple and inexpensive route for PANI/clay nanofibers for the first time is well established. Fibrous morphology is evident from SEM pictures

where the high polymer order and crystallinity is clear from X-ray diffraction patterns. FTIR and UV-DRS spectral analysis shows the strong interaction between PANI and PILC that gives additional stability to the intercalated polymer within the matrix, clear from the DTG analysis. The composite is having good conductivity, but less than that of pure PANI, due to the weakening in interchain interactions within the confined matrix.

Reference

1. Focke, W. W.; Wnek, G. E.; Wei, Y. J Phys Chem 1987, 91, 5813.
2. Kingsborough, R. P.; Swager, T. M. Adv Mater 1998, 10, 1100.
3. Riede, A.; Helmstedt, J.; Riede, V.; Zemek, J.; Stejskal, J. Langmuir 2000, 16, 6240.
4. Goller, M. I.; Barthet, C.; McCarthy, G. P.; Corradi, R.; Newby, B. P.; Wilson, S. A.; Armes, S. P.; Luk, S. Y. Colloid Polym Sci 1998, 276, 1010.
5. Kim, J. W.; Kim, S. G.; Choi, H. J.; John, M. S. Macromol Rapid Commun 1999, 20, 450.
6. Kong, J.; Franklin, N. R.; Zhou, C.; Chapline, M. G.; Peng, S.; Cho, K.; Dai, H. Science 2000, 287, 622.
7. Chen, K. H.; Yang, S. M. Synth Met 2003, 135/136, 151.
8. Wu, Q.; Qi, Z.; Wang, F. Polymer 2000, 41, 2029.
9. Lee, D.; Char, K. Polym Degrad Stabil 2002, 75, 555.
10. Orata, D.; Segor, F. React Funct Polym 2000, 43, 305.
11. Lim, Y. T.; Park, J. H.; Park, O. O. J. Colloid Interface Sci 2002, 245, 198.
12. Kim, B. H.; Jung, J. H.; Kim, J. W.; Choi, H. J.; Joo, J. Synth Met 2001, 117, 115.
13. Kim, J. W.; Kim, S. G.; Choi, H. J.; John, M. S. Macromol Rapid Commun 1999, 20, 450.
14. Allcock, H. R. Science 1992, 255, 1106.
15. Giannelis, E. P. Adv Mater 1996, 8, 29.
16. Jagtap, N.; Ramaswamy, V. Appl Clay Sci 2006, 33, 89.
17. Figueras, F. Catal Rev Sci Eng 1988, 30, 457.
18. Geatti, A.; Lenarda, M.; Storaro, L.; Ganzerla, R.; Perissinotto, M. J Mol Catal A: Chem 1997, 121, 111.
19. Pinnavaia, T. J.; Tzou, M. S.; Landau, S. D. J Am Chem Soc 1985, 107, 4785.
20. Pillared, C.; Burch, R., Eds. Catalysis Today; Elsevier: New York, 1988; Vol. 2, p 289.
21. Avlyanov, J. K.; Josefowicz, J. Y.; MacDiarmid, A. G. Synth Met 1995, 73, 205.
22. Chandrasekhar, P. Conducting Polymers, Fundamentals and Applications: A Practical Approach; Kluwer Academic: Boston, 1999.
23. Zhang, X.; Manohar, S. K. Chem Commun, 2004, 2360.
24. Li, J.; Fang, K.; Qiu, H.; Li, S. P.; Mao, W. M. Synth Met, 2004, 142, 107.
25. Li, J.; Fang, K.; Qiu, H.; Li, S. P.; Mao, W. M.; Wu, Q. Synth Met 2004, 145, 191.
26. Sui, X.; Chu, Y.; Xing, S.; Liu, C. Mater Lett 2004, 25, 1255.
27. Pouget, J. P.; Jozefowicz, M. E.; Epstein, A. J.; Tang, X.; Macdiarmid, A. G. Macromolecules 1991, 24, 779.

28. Nalwa, H. S., Ed. Handbook of Conductive Molecules and Polymers: Conductive Polymers. Synthesis and Electrical Properites; Wiley: India, 1997; Vol. 2, p 506.
29. Quillard, S.; Louran, G.; Lefrant, S.; Mac Diarmid, A. G. Phys Rev B 1994, 50, 12496.
30. Kim, B. H.; Jung, J. H.; Hong, S. H.; Joo, J. Macromolecules 2002, 35, 1419.
31. Lu, F. L.; Wudll, F.; Nowak, M.; Heeger, A. J. J Am Chem Soc 1986, 108, 8311.
32. Stafstrom, S.; Breadas, J. L.; Epstein, A. J.; Woo, H. S.; Tenner, D. B.; Huang, W. S.; Macdiarmid, A. G. Phys Rev Lett 1987, 59, 1464.
33. Mac Diarmid, A. G.; Huang, W. S. Polymer 1993, 34, 1833.
34. Hatano, T.; Bae, A. H.; Takeuchi, M.; Ikeda, A.; Shinkai, S. Bull Chem Soc Jpn 2004, 77, 1951.
35. Alan, G. M.; Arthur, J. E. Synth Met 1995, 69, 85.
36. Wu, Q.; Xue, Z.; Qi, Z.; Wang, F. Polymer 2000, 41, 2029.
37. Chan, H. S. O.; Teo, M. T. B.; Khor, E.; Lim, C. N. J Therm Anal 1989, 35, 765.
38. Neoh, K. G.; Kang, E. T.; Tan, K. L. Thermochim Acta 1990, 171, 279.
39. Lee, D.; Char, K. Polym Degrad Stabil 2002, 75, 555.
40. Bae, W. J.; Kim, K. H.; Jo, W. H. Macromolecules 2004, 37, 9850.